Nanoscale Advances

ROYAL SOCIETY OF CHEMISTRY

PAPER

View Article Online
View Journal | View Issue

Cite this: *Nanoscale Adv.*, 2023, **5**, 725

Mechanical tough and multicolor aggregation-induced emissive polymeric hydrogels for fluorescent patterning†

Yi Zhang,[ab] Ruijia Wang,[b] Wei Lu, *[b] Wanning Li,[b] Si Chen *[a] and Tao Chen *[b]

Received 30th October 2022
Accepted 13th December 2022

DOI: 10.1039/d2na00757f

rsc.li/nanoscale-advances

Aggregation-induced emissive fluorogens (AIEgens) are promising building blocks for fluorescent polymeric hydrogels (FPHs) because intense fluorescence intensities are usually guaranteed by spontaneous aggregates of hydrophobic AIEgens in a hydrophilic polymer network. However, most AIE-active FPHs are single-color fluorescent and cannot display tunable emission colors. Additionally, efforts to produce mechanically strong AIE-active hydrogels have been largely ignored, restricting their potential uses. Herein, we present the synthesis of an AIE-active methyl picolinate-substituted 1,8-naphthalimide monomer (MP-NI) for fabricating mechanical tough and multicolor FPHs. Owing to the introduction of bulky and coordinative methyl picolinate group, these specially designed MP-NI molecules were forced to adopt propeller-shaped conformation that renders them with intense aggregation-induced blue emission. Moreover, the MP-NI moieties grafted in a hydrogel matrix can sensitize red and green fluorescence of $Eu^{3+}$and Tb^{3+} *via* antenna effect. Consequently, multicolor fluorescent hydrogels that sustain a high stress of 1 MPa were obtained by chemically introducing MP-NI moieties into dually cross-linked alginate polymer networks with high-density metal (Ca^{2+}/Tb^{3+}/Eu^{3+}) coordination and hydrogen bonding crosslinks. Their capacity to enable the writing of arbitrary multicolor fluorescent patterns using Eu^{3+}/Tb^{3+} as inks were finally demonstrated, suggesting their potential uses for smart display and information encryption.

Introduction

Fluorescent polymeric hydrogels (FPHs) are the rising stars of luminescent materials, which can combine the merits of traditional fluorescent polymers and hydrogels, including responsive fluorescence, tissue-like modulus, and intrinsic soft wet nature.[1–6] These advantages make FPHs potentially useful for various applications ranging from bioimaging and sensing[7,8] to information encryption[9–11] and soft robotics.[12–15] The past two decades have witnessed the development of numerous FPHs based on organic fluorophores,[16–24] luminescent metal complexes[25–32] and nanoparticles.[33–36] Aggregation-induced emissive fluorogens (AIE-gens) are attracting increasing research attention[37–40] because hydrophobic AIE-gens are self-assembled into highly luminescent aggregates in hydrophilic hydrogel matrix, which is guaranteed to produce FPHs with intense fluorescence.[41–43] For example, Yang *et al.* presented a series of various colored fluorescent hydrogels with intense aggregation-induced emission by physically introducing tetraphenyl ethylene or its derivative into poly(vinyl alcohol) hydrogels.[44] We have developed a number of highly fluorescent FPHs *via* the radical copolymerization of AIE-active hydrophobic naphthalimide derivatives into cross-linked hydrophilic polymer network.[45,46] These recent advances have largely enriched the family of AIE-active hydrogels and laid a solid foundation for future applications.

These reported AIE-active FPHs, albeit state-of-the-art, are found to be primarily single-color fluorescent and fail to display tunable emission colors that are more promising for many uses. The synthesis of multicolor aggregation-induced emissive hydrogels is thus desired but seems quite challenging.[47] To do this, an ideal approach is to directly introduce one single AIE-gen with responsive emission color changes into cross-linked polymer networks, but such AIE-gens are quite few and usually have a limited color change range. Another possible approach is through the pair use of two or more responsive AIE-gens in the hydrogel system. However, a careful choice of AIE-gen pairs is always necessary by elaborately investigating the complex photophysical interactions between different luminogens as well as their compatibility in one single hydrogel matrix. Additionally, most reported FPHs still suffer from

[a]*College of Material Science and Engineering, Zhejiang University of Technology, Hangzhou 310014, Zhejiang, China. E-mail: chensi@zjut.edu.cn*

[b]*Key Laboratory of Marine Materials and Related Technologies, Zhejiang Key Laboratory of Marine Materials and Protective Technologies, Ningbo Institute of Materials Technology and Engineering, Chinese Academy of Sciences, Ningbo 315201, China. E-mail: luwei@nimte.ac.cn; tao.chen@nimte.ac.cn*

† Electronic supplementary information (ESI) available. See DOI: https://doi.org/10.1039/d2na00757f

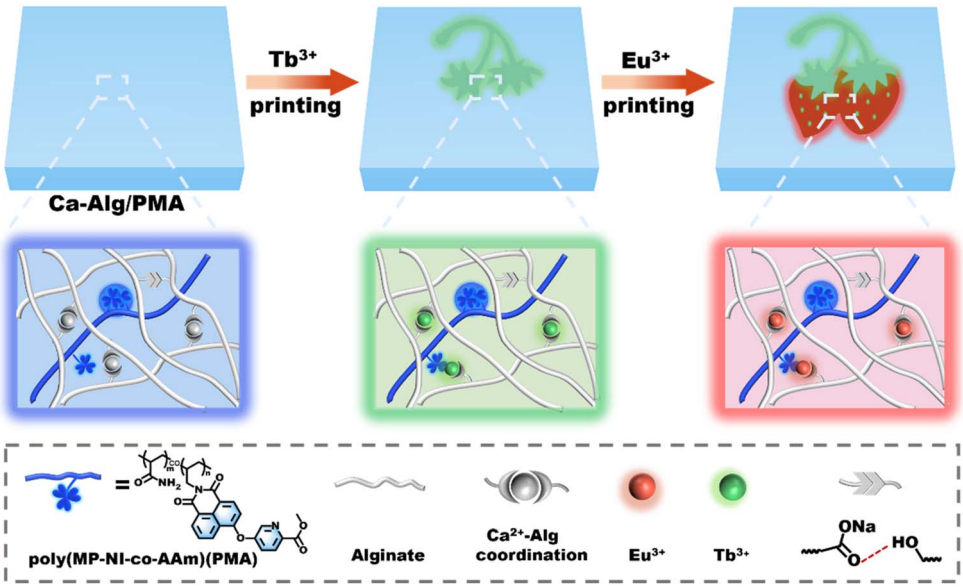

Scheme 1 Schematic illustration showing the chemical structure of the designed aggregation-induced emissive polymeric hydrogels, and the procedure to achieve multicolor fluorescent patterning. The AIE-active Ca-Alg/PMA hydrogels with intense blue emission and mechanical toughness were prepared by incorporating the hydrophilic PMA polymer into the dually cross-linked Alg polymer networks with high-density Ca^{2+} coordination and hydrogen bonding crosslinks. Because Tb^{3+}/Eu^{3+} ions have stronger coordination capacity than Ca^{2+}, green and red fluorescent patterns could be facilely written on the Ca-Alg/PMA hydrogels using the Tb^{3+}/Eu^{3+} inks to break the Ca^{2+} complexes to form green and red fluorescent Tb^{3+} and Eu^{3+} complexes.

relatively weak mechanical stress and few systems can sustain a fracture stress of over 0.5 MPa. Therefore, it is still challenging to develop multicolor aggregation-induced emissive polymeric hydrogels with tough mechanical strength.

Herein, we propose to develop a unique type of hydrophobic AIE-gens with coordinative methyl picolinate groups, which emit intense blue fluorescence and sensitize Tb^{3+} and Eu^{3+} luminescence to form green and red fluorescent centers in a single hydrogel system. As illustrated in Scheme 1, when the hydrophobic AIE-active methyl picolinate-substituted 1,8-naphthalimide monomer (MP-NI) was first copolymerized into hydrophilic poly(MP-NI-*co*-Acrylamide) (PMA) polymer and then incorporated in the dually cross-linked alginate (Alg) polymer networks with high-density Ca^{2+} coordination and hydrogen bonding crosslinks, AIE-active Ca-Alg/PMA hydrogels with intense blue emission and mechanical toughness were obtained. Similarly, green and red fluorescent Tb-Alg/PMA and Eu-Alg/PMA hydrogels could be prepared, respectively, using Tb^{3+} and Eu^{3+} ions to crosslink the Alg and PMA polymer network. Consequently, multicolor fluorescent patterns were capable of being facilely written or printed on the Ca-Alg/PMA hydrogels using aqueous Tb^{3+} or Eu^{3+} solutions as the inks. This is because Tb^{3+}/Eu^{3+} ions have stronger coordination capacity than Ca^{2+} and easily broke the Ca^{2+} complexes to form green and red fluorescent Tb^{3+} and Eu^{3+} complexes. Such facile capacity to construct arbitrary multicolor fluorescent patterns has been rarely achieved but is appealing for potential information display or encryption uses.

Results and discussion

Fig. 1a depicts the synthetic route for the AIE-active methyl picolinate-substituted 1,8-naphthalimide monomer (MP-NI). *N*-allyl-4-bromonaphthalimide was first prepared using the reported method[45] and then allowed to react with methyl 4-hydroxypicolinate to produce MP-NI as a yellow solid. Its chemical structure and purity were verified by ^{1}H NMR, ^{13}C NMR, ESI-MS and FT-IR spectra (Fig. S1†). As can be observed from the NMR spectra shown in Fig. 1b and c, the evident proton signal at 4.0 ppm and carbon signal at 53.4 ppm indicates the successful substitution of methyl picolinate moieties. There exists only one intense peak in the ESI-MS spectrum, suggesting high purity of the obtained monomer (Fig. 1d). MP-NI is insoluble in water but rapidly solves in common organic solvents, such as ethanol, $CHCl_3$, THF, DMSO and DMF. Its UV-vis spectrum exhibited a strong absorption band around 350 nm (Fig. S2†), suggesting that its fluorescence can be excited by low-energy UV light (*e.g.*, 365 nm). Owing to the introduction of bulky methyl picolinate substituent group, the MP-NI molecule was forced to adopt a propeller-shaped conformation that may consume a certain amount of energy *via* dynamic intramolecular vibrations and rotations in good solution.[48,49] Therefore, its THF solution is moderately fluorescent. However, the blue emission intensity could be further enhanced with increasing content of H_2O to induce the gradual formation of hydrophobic MP-NI aggregates, in which the intramolecular rotations and vibration were largely restricted. As shown in Fig. 1e and f, the emission intensity at 428 nm

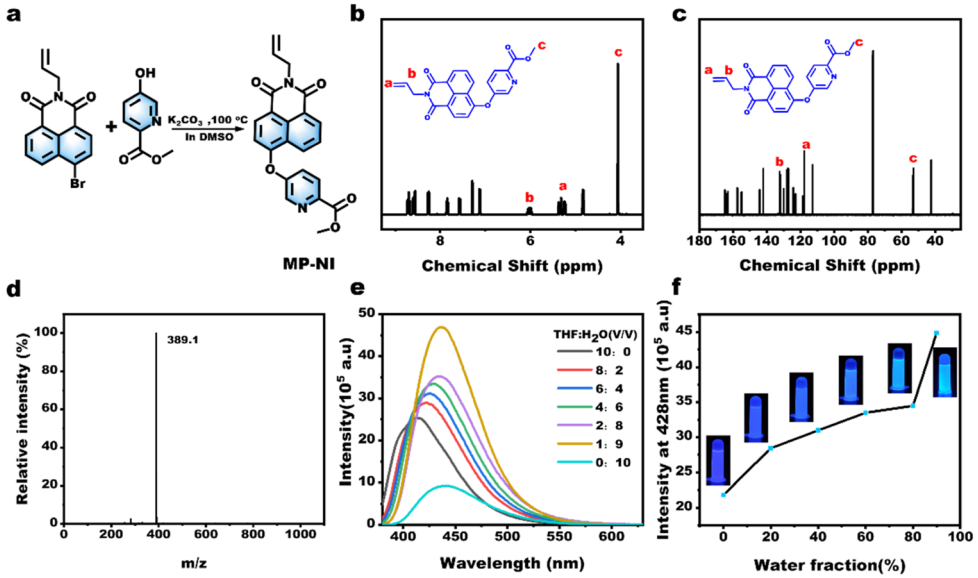

Fig. 1 (a) Synthetic procedure of the AIE-active MP-NI monomer; (b) ^{1}H NMR and (c) ^{13}C NMR spectra of MP-NI recorded in $CDCl_3$; (d) electron spray ionization mass spectrometry of MP-NI. (e) Fluorescence spectra of MP-NI in mixed THF/H_2O solutions when excited at 365 nm; (f) peak fluorescence intensity of MP-NI as a function of the water content in THF/H_2O mixtures (inset photos showing fluorescence of MP-NI in mixed THF/H_2O solutions taken under 365 nm UV lamp).

gradually increased and reached the maximum at 90 vol% water content. These results suggested the typical aggregation-induced emission enhancement nature of the newly designed MP-NI monomer. To facilitate the synthesis of fluorescent polymeric hydrogel, this hydrophobic MP-NI monomer was next radically copolymerized with acrylamide (AAm) in 1,4-dioxane to produce the hydrophilic poly(MP-NI-*co*-Acrylamide) (PMA) polymer (Fig. 2a and S3†). Owing to the low polymerization activity of MP-NI monomer, it is essential to completely remove the residual fluorescent monomer to obtain high-purity PMA polymer. To do this, the polymerized solution was poured into a large amount of hexane to precipitate the polymer. TLC experiment was further used to demonstrate that there was indeed no MP-NI residue in the collected polymer (Fig. S4†). The hydrophobic MP-NI content was very slight in the polymer, but PMA was still readily soluble in water. Fig. 2b summarizes the UV-vis and fluorescence spectra of aqueous solution of PMA. The existence of clear absorption peak around 271 nm further indicated the covalent incorporation of MP-NI into the polymer. Because of the spontaneous aggregation of hydrophobic MP-NI moieties, its aqueous solution is highly blue fluorescent. Further fluorescence spectral changes of PMA recorded in the mixture of water (good solvent) and ethanol (bad solvent) demonstrated the AIE-active nature of this polymer (Fig. 2c and d). Based on blue fluorescent polymer with aggregation-induced emission enhancement characteristics, highly fluorescent polymeric hydrogels could be facilely constructed by introducing PMA into cross-linked polymer network. To simultaneously improve mechanical strength, sodium alginate (Alg) polymer bearing high-density –OH and COO^- groups was used as the hydrogel matrix. Fig. 3a depicts the proposed synthetic procedure, in which mixed solution of PMA and Alg were first prepared and then cross-liked by the addition of Ca^{2+} ions. During the gelation process, vast hydrogen bonds were formed between PMA and Alg polymer chains, making PMA evenly and stably distributed in the hydrogel matrix. Moreover, strong Ca^{2+} coordination crosslinks with the COO^- groups of Alg were also formed, as evidenced by the characteristic peaks at 351.2 eV (Ca $2p_{1/2}$) and 347.0 eV (Ca $2p_{3/2}$) in the XPS spectra (Fig. 3b). Owing to the coexistence of hydrogen bonded and metal coordinated polymer networks, the obtained Ca-Alg/PMA hydrogel proved to

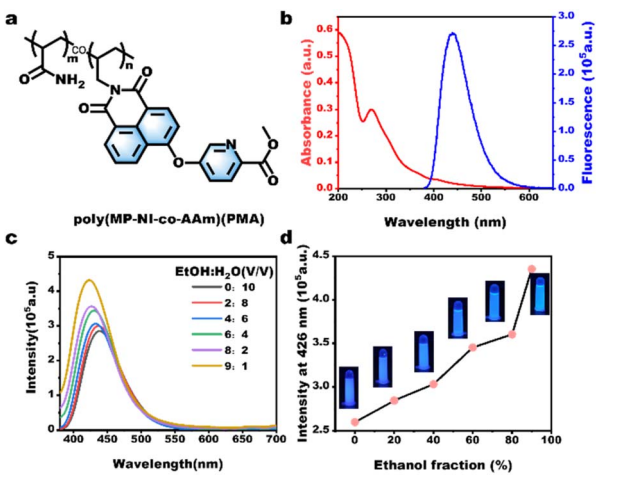

Fig. 2 (a) Chemical structure of poly(MP-NI-*co*-AAm); (b) UV-vis and fluorescence spectra of aqueous PMA solution (0.01 M); (c) fluorescence spectra of PMA in mixed ethanol/H_2O solutions when excited at 365 nm; (d) peak fluorescence intensity of PMA as a function of the water content in mixed ethanol/H_2O solutions (inset photos showing fluorescence of PMA in mixed ethanol/H_2O solutions taken under 365 nm UV lamp).

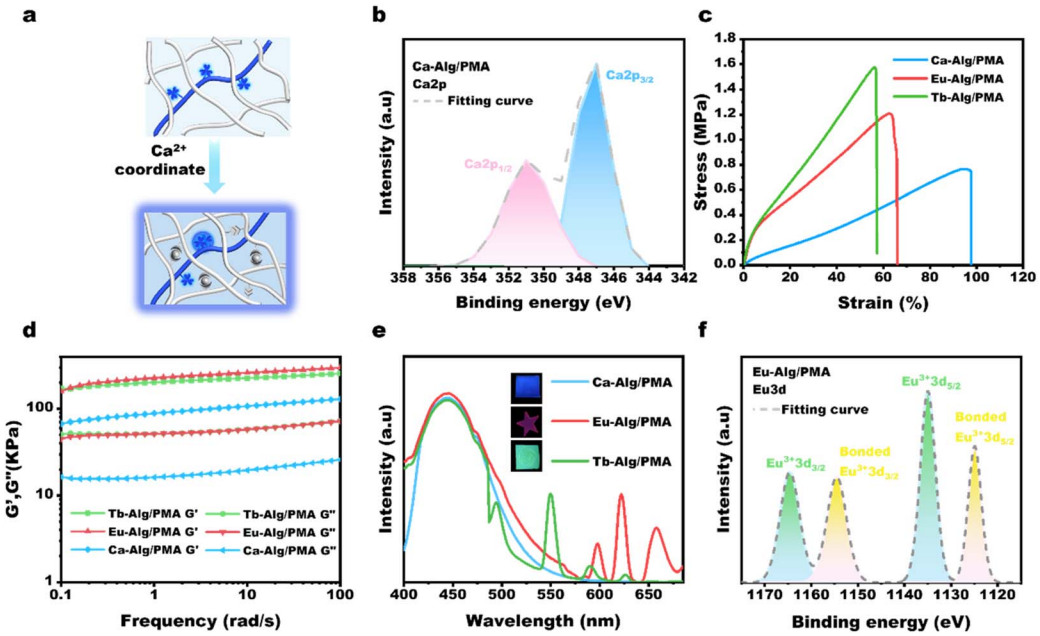

Fig. 3 (a) Scheme showing the preparation of dually cross-linked Ca-Alg/PMA hydrogels with Ca^{2+} coordination and hydrogen bonding crosslinks. (b) High-resolution XPS fitting spectra of Ca 2p; (c) tensile stress–strain curves; (d) rheology properties of Ca-Alg/PMA, Eu-Alg/PMA and Tb-Alg/PMA hydrogels at 1% strain; (e) normalized fluorescence spectra of the Eu-Alg/PMA, Tb-Alg/PMA and Ca-Alg/PMA hydrogels; and (f) high-resolution XPS fitting spectra of Eu 3d.

sustain a fracture strain of ~100% and a moderate stress of ~0.8 MPa (Fig. 3c), which is nearly comparable to that of natural skeletal muscles (~1 MPa). Additionally, intense blue fluorescence was observed for Ca-Alg/PMA hydrogel because of the formed hydrophobic MP-NI aggregates in the hydrophilic hydrogel matrix (Fig. 3e). For enriching fluorescence colors and toughening the mechanical strength of the obtained hydrogels, Tb-Alg/PMA and Eu-Alg/PMA hydrogels were fabricated *via* a similar method (Fig. S5†). In these hydrogels, Tb^{3+} and Eu^{3+} ions with stronger coordination capacity than Ca^{2+} were utilized to crosslink the PMA and Alg polymer chains. SEM images of the obtained Eu-Alg/PMA and Tb-Alg/PMA hydrogel samples indicated a porous crosslinking structure (Fig. S6†). As can be observed from the XPS results shown in Fig. 3f, the peaks of Eu $3d_{3/2}$ and Eu $3d_{5/2}$ shifted toward the lower binding energy. This result demonstrated that Eu^{3+} shared electron pairs with the COO^- groups of Alg and pyridine groups of PMA through lanthanide-ligand coordination interactions in the obtained Eu-Alg/PMA. Similar XPS results were observed for the Tb-Alg/PMA hydrogel (Fig. S7†). Because of these strong lanthanide coordination crosslinks, the mechanical strengths of the obtained Tb-Alg/PMA and Eu-Alg/PMA hydrogels were further enhanced compared with the Ca-Alg/PMA hydrogel. The results shown in Fig. 3c revealed that Tb-Alg/PMA and Eu-Alg/PMA hydrogels could sustain a high stress of more than 1 MPa, which is much higher than most of the reported fluorescent polymeric hydrogels. However, the fracture strain maintained about 70%, which was lower than Ca-Alg/PMA because of higher lanthanide

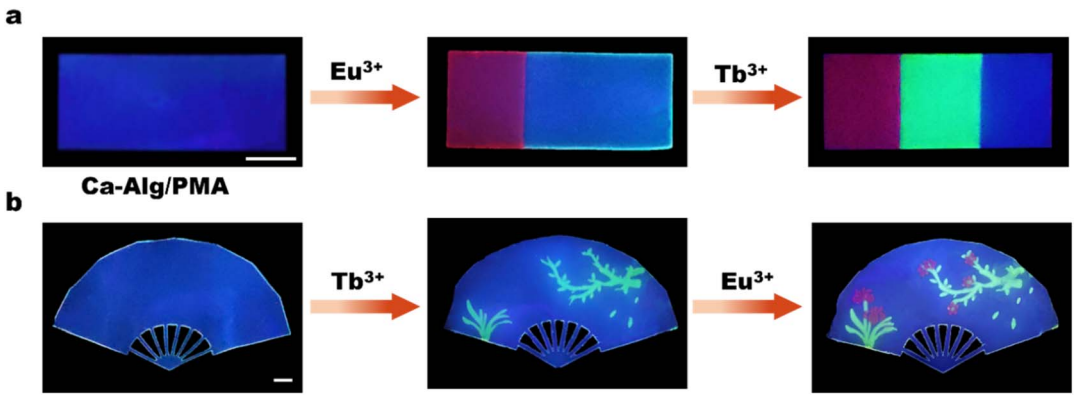

Fig. 4 Fabrication of multicolor fluorescent patterns on the Ca-Alg/PMA hydrogel sheet by using (a) Eu^{3+}/Tb^{3+} ions or (b) Tb^{3+}/Eu^{3+} ions as the inks.

coordination strength. Similarly, Eu-Alg/PMA and Tb-Alg/PMA hydrogels have higher modulus and toughness than Ca-Alg/PMA hydrogel, clearly demonstrating the formation of strong lanthanide coordination crosslinks (Fig. 3d). Moreover, the luminescence intensities of Tb^{3+} and Eu^{3+} ions were remarkably sensitized by the coordinated COO^- and methyl picolinate chromophores *via* resonance energy transfer (RET). As evidenced from the fluorescence spectra in Fig. 3e, additional green and red emission bands also appeared, respectively. The fluorescence spectra recorded in the Eu-Alg/PMA gels with increasing water fraction from 0% to 100% in the ethanol/water gel matrix suggested the AIE-active nature of Eu-Alg/PMA hydrogel (Fig. S8†). Their UV-vis spectra have also been conducted (Fig. S9†).

Having obtained the mechanically strong and multicolor fluorescent hydrogels, we explored the possibility to produce multicolor fluorescent patterns, which may find broad applications in smart displays, information encryption and so on. To this end, the Tb^{3+} or Eu^{3+} ink was brushed on Ca-Alg/PMA hydrogel sheet, instantly transforming the initially blue fluorescence to green or red color (Fig. 4a, b and S10†). This is because Tb^{3+} and Eu^{3+} ions with stronger coordination capacity could break the Ca^{2+} complexes and induce the formation of more Ca^{2+} complexes and induce the formation of more stable lanthanide complexes through metal ion replacement. Similarly, various types of multicolor fluorescent patterns could be facilely written or printed on the Ca-Alg/PMA hydrogel sheet using Tb^{3+} and Eu^{3+} ions as the inks, suggesting many potential applications.

Conclusions

In conclusion, we demonstrated a robust kind of mechanical tough and multicolor aggregation-induced emissive alginate hydrogels based on one specially designed AIE-active MP-NI monomer containing coordinative methyl picolinate group. The hydrogel materials were constructed by first copolymerizing hydrophobic MP-NI moieties into the hydrophilic poly(MP-NI-*co*-AAm) chain and then co-gelation of poly(MP-NI-*co*-AAm) and alginate solutions through high-density metal (Ca^{2+}, Tb^{3+} or Eu^{3+}) coordination and hydrogen bonding interactions. Mechanical toughness of these as-prepared alginate hydrogels were thus guaranteed by the dually cross-linked polymer networks. Owing to the spontaneous MP-NI aggregation in hydrophilic polymer network, the as-prepared Ca-Alg/PMA hydrogels were highly blue fluorescent. Different from Ca-Alg/PMA hydrogels, Tb-Alg/PMA and Eu-Alg/PMA hydrogels were found to display additional green and red emission bands. This is because Tb^{3+} and Eu^{3+} luminescence could be sensitized by the coordinated COO^- and methyl picolinate chromophores grafted in the hydrogel matrix. Based on the established multicolor and tough hydrogels, we further demonstrated the possibility to write arbitrary colorful fluorescent patterns on the Ca-Alg/PMA hydrogel sheet using Tb^{3+} and Eu^{3+} with stronger coordination capacity as the inks. Because of their modular design principle and capacity for fabricating various multicolor fluorescent patterns, these AIE-active hydrogels are expected to find many potential uses in smart display and information encryption.

Experimental details

Materials

Acrylamide (AAm, ≥98.0%), potassium carbonate (K_2CO_3, ≥99.0%), ethyl alcohol (EtOH, ≥99.7%), tetrahydrofuran (THF, ≥95.0%), dichloromethane (CH_2Cl_2, ≥99.5%) and sodium hydrogen carbonate ($NaHCO_3$, ≥99.5%) were purchased from Sinopharm Chemical Reagent Co., Ltd. Sodium alginate (viscosity 200 ± 20 mpa s), anhydrous calcium chloride ($CaCl_2$, 96.0%), anhydrous sodium sulfate (Na_2SO_4, 99%), methyl 5-hydroxypyridine-2-carboxylate (97%), dimethyl sulfoxide (DMSO), 1,4-dioxane (≥99.5%), $Eu(NO_3)3\cdot 6H_2O$ (99.9%), $Tb(NO_3)_3\cdot 5H_2O$ (99.9%) and 2, 2-azo diisobutyronitrile (AIBN, 99%) were obtained from Aladdin Chemistry Co. Ltd. 4-Bromo-1, 8-naphthalene anhydride (≥97%) were gotten from Afaisha (China) Chemical Co., Ltd. Allylamine hydrochloride was purchased from TCI (Shanghai) Development Co., Ltd. 2, 2-azo diisobutyronitrile were used after crystallization.

Synthesis of fluorescent monomer (MP-NI)

4-Bromo-*N*-allyl-1,8-naphthalimide was previously synthesized based on a reported method.[45] Methyl 5-hydroxypyridine-2-carboxylate (0.3092 g, 2.02 mmol), K_2CO_3 (0.828 g, 6 mmol) and 4-bromo-*N*-allyl-1,8-naphthalimide (0.632 g, 2 mmol) were dissolved in 60 mL DMSO in a 250 mL three neck flask under N_2 protection. Then, the reaction mixture was continuously stirred for 12 h at 100 °C. After being cooled to room temperature, 200 mL water was added, and the mixture was then extracted by CH_2Cl_2 for three times to obtain the product solution. Next, anhydrous sodium sulfate was added to the product solution to remove the residual water. After removing the organic phase under a vacuum, the obtained solid was washed with deionized water to remove the residual reactants. Finally, MP-NI monomer was obtained as a yellow powder after being dried under vacuum in 50.95% yield.

Synthesis of linear poly(MP-NI-*co*-AAm) (PMA) polymer

Under N_2 atmosphere, AAm (2 g), MP-NI monomer (0.02 g, 1 wt% of the AAm monomer) and AIBN (0.02 g) were dissolved in 80 mL 1,4-dioxane. After being polymerized at 65 °C for 8 h, the mixture was added to hexane (150 mL) dropwise to precipitate the linear polymer. After being dried under vacuum for 6 h, PMA was obtained as a white solid.

Preparation of Ca-Alg/PMA, Ca-Alg/PMA, and Ca-Alg/PMA hydrogels

Sodium alginate (Alg, 4 g) and linear PMA polymer (0.2 g) were first dissolved in deionized water (100 mL) to obtain a viscous solution. The 9 g solution was added into the self-made molds consisting of one quartz glass plate and two 1 mm-thick PDMS films on it. Then, 8 mL aqueous solution of Ca^{2+} (0.3 M) was injected on the top side of the viscous Alg/PMA solution. After

1 h, the Ca-Alg/PMA hydrogel was obtained. Eu-Alg/PMA and Tb-Alg/PMA hydrogels were obtained using a similar method.

Characterization

^{1}H NMR and ^{13}C NMR spectra were recorded on a Bruker Avance III 400 MHz spectrometer in $CDCl_3$. UV-vis absorption spectra were measured on a UV-vis spectrophotometer (TU-1810, Purkinje General Instrument Co., Ltd). Steady-state fluorescence measurements were obtained using a fluorescence spectrofluorometer (FL3-111) at room temperature. Surface morphology of the freeze-dried Eu-Alg/PMA hydrogel sample was performed by field-emission scanning electron microscopy (SEM, S-4800, Hitachi) with an accelerating voltage of 4.0 kV. Tensile tests of these hydrogels were conducted on a Zwick Roell Z1.0 universal material testing machine. The strip samples with a size of 30 mm × 10 mm × 1 mm with a crosshead distance of 10 mm were stretched at a constant speed (30 mm min^{-1}). Dynamic rheological measurements were characterized by a stress-controlled rheometer (Physica MCR-301, Anton Paar) to obtain the frequency sweep (strain = 1%) spectra of hydrogels with 25 mm parallel plates.

Author contributions

W. L., S.·C., and T. C. designed this study. Y. Z., R. J. W and W.N. L. performed the experiments.

Conflicts of interest

The authors declare no competing financial interest.

Acknowledgements

We gratefully acknowledge the National Natural Science Foundation of China (52073297), the Youth Innovation Promotion Association of Chinese Academy of Sciences (2019297), Ningbo Natural Science Foundation (2021J194), and the K. C. Wong Education Foundation (GJTD-2019-13).

Notes and references

1 B. Li, T. He, X. Shen, D. Tang and S. Yin, Fluorescent supramolecular polymers with aggregation induced emission properties, *Polym. Chem.*, 2019, **10**, 796–818.
2 D. Li, J. Wang and X. Ma, White-Light-Emitting Materials Constructed from Supramolecular Approaches, *Adv. Opt. Mater.*, 2018, **6**, 1800273.
3 Y. Li, D. J. Young and X. J. Loh, Fluorescent gels: a review of synthesis, properties, applications and challenges, *Mater. Chem. Front.*, 2019, **3**, 1489–1502.
4 Z. Li, X. Ji, H. Xie and B. Z. Tang, Aggregation-Induced Emission-Active Gels: Fabrications, Functions, and Applications, *Adv. Mater.*, 2021, **33**, e2100021.
5 H. Wang, X. Ji, Z. Li and F. Huang, Fluorescent Supramolecular Polymeric Materials, *Adv. Mater.*, 2017, **29**, 1606117.
6 W. Lu, M. Si, X. Le and T. Chen, Mimicking Color-Changing Organisms to Enable the Multicolors and Multifunctions of Smart Fluorescent Polymeric Hydrogels, *Acc. Chem. Res.*, 2022, **55**, 2291–2303.
7 J. Zhong, T. Zhao and M. Liu, Fluorescence microscopic visualization of functionalized hydrogels, *NPG Asia Mater.*, 2022, **14**, 38.
8 N. Mehwish, X. Dou, Y. Zhao and C. L. Feng, Supramolecular fluorescent hydrogelators as bio-imaging probes, *Mater. Horiz.*, 2019, **6**, 14–44.
9 C. N. Zhu, T. Bai, H. Wang, J. Ling, F. Huang, W. Hong, Q. Zheng and Z. L. Wu, Dual-Encryption in a Shape-Memory Hydrogel with Tunable Fluorescence and Reconfigurable Architecture, *Adv. Mater.*, 2021, **33**, e2102023.
10 H. Shi, S. Wu, M. Si, S. Wei, G. Lin, H. Liu, W. Xie, W. Lu and T. Chen, Cephalopod-Inspired Design of Photomechanically Modulated Display Systems for On-Demand Fluorescent Patterning, *Adv. Mater.*, 2022, **34**, e2107452.
11 K. Lou, Z. Hu, H. Zhang, Q. Li and X. Ji, Information Storage Based on Stimuli-Responsive Fluorescent 3D Code Materials, *Adv. Funct. Mater.*, 2022, **32**, 2113274.
12 C. Ma, W. Lu, X. Yang, J. He, X. Le, L. Wang, J. Zhang, M. J. Serpe, Y. Huang and T. Chen, Bioinspired Anisotropic Hydrogel Actuators with On-Off Switchable and Color-Tunable Fluorescence Behaviors, *Adv. Funct. Mater.*, 2018, **28**, 1704568.
13 L. Hu, Y. Wan, Q. Zhang and M. J. Serpe, Harnessing the Power of Stimuli-Responsive Polymers for Actuation, *Adv. Funct. Mater.*, 2019, **30**, 1903471.
14 C. Yang, F. Su, Y. Xu, Y. Ma, L. Tang, N. Zhou, E. Liang, G. Wang and J. Tang, pH Oscillator-Driven Jellyfish-like Hydrogel Actuator with Dissipative Synergy between Deformation and Fluorescence Color Change, *ACS Macro Lett.*, 2022, **11**, 347–353.
15 J. Fang, Y. Zhuang, K. Liu, Z. Chen, Z. Liu, T. Kong, J. Xu and C. Qi, A Shift from Efficiency to Adaptability: Recent Progress in Biomimetic Interactive Soft Robotics in Wet Environments, *Adv. Sci.*, 2022, **9**, e2104347.
16 X. Ji, R. T. Wu, L. Long, X. S. Ke, C. Guo, Y. J. Ghang, V. M. Lynch, F. Huang and J. L. Sessler, Encoding, Reading, and Transforming Information Using Multifluorescent Supramolecular Polymeric Hydrogels, *Adv. Mater.*, 2018, **30**, 1705480.
17 Y. Lin, C. Li, G. Song, C. He, Y. Q. Dong and H. Wang, Freezing-induced multi-colour emissions of AIE luminogen di(4-propoxyphenyl) dibenzofulvene, *J. Mater. Chem. C*, 2015, **3**, 2677–2685.
18 D. Lu, M. Zhu, S. Wu, Q. Lian, W. Wang, D. Adlam, J. A. Hoyland and B. R. Saunders, Programmed Multiresponsive Hydrogel Assemblies with Light-Tunable Mechanical Properties, Actuation, and Fluorescence, *Adv. Funct. Mater.*, 2020, **30**, 1909359.
19 W. Yuan, J. Cheng, X. Li, M. Wu, Y. Han, C. Yan, G. Zou, K. Mullen and Y. Chen, 5,6,12,13-Tetraazaperopyrenes as Unique Photonic and Mechanochromic Fluorophores, *Angew. Chem., Int. Ed.*, 2020, **59**, 9940–9945.

20 K. Benson, A. Ghimire, A. Pattammattel and C. V. Kumar, Protein Biophosphors: Biodegradable, Multifunctional, Protein-Based Hydrogel for White Emission, Sensing, and pH Detection, *Adv. Funct. Mater.*, 2017, **27**, 1702955.

21 R. Merindol, G. Delechiave, L. Heinen, L. H. Catalani and A. Walther, Modular Design of Programmable Mechanofluorescent DNA Hydrogels, *Nat. Commun.*, 2019, **10**, 528.

22 X. F. Li, W. Zhou, Y. C. Liu, M. Hou, G. L. Feng, Y. M. Ji, Y. Zhang and G. W. Xing, Design and assembly of AIE-active fluorescent organic nanoparticles for anti-counterfeiting fluorescent hydrogels and inks, *Chem. Commun.*, 2022, **58**, 11547–11550.

23 J. M. Galindo, J. Leganes, J. Patino, A. M. Rodriguez, M. A. Herrero, E. Diez-Barra, S. Merino, A. M. Sanchez-Migallon and E. Vazquez, Physically Cross-Linked Hydrogel Based on Phenyl-1,3,5-triazine: Soft Scaffold with Aggregation-Induced Emission, *ACS Macro Lett.*, 2019, **8**, 1391–1395.

24 F. Yang, X. Li and Y. Chen, A Chromic and Near-Infrared Emissive Melanophore Serving as a Versatile Force Meter in Micelle–Hydrogel Composites, *Adv. Opt. Mater.*, 2022, **10**, 2102552.

25 Q. F. Li, X. Du, L. Jin, M. Hou, Z. Wang and J. Hao, Highly luminescent hydrogels synthesized by covalent grafting of lanthanide complexes onto PNIPAM *via* one-pot free radical polymerization, *J. Mater. Chem. C*, 2016, **4**, 3195–3201.

26 Z. Li, H. Chen, B. Li, Y. Xie, X. Gong, X. Liu, H. Li and Y. Zhao, Photoresponsive Luminescent Polymeric Hydrogels for Reversible Information Encryption and Decryption, *Adv. Sci.*, 2019, **6**, 1901529.

27 K. Meng, C. Yao, Q. Ma, Z. Xue, Y. Du, W. Liu and D. Yang, A Reversibly Responsive Fluorochromic Hydrogel Based on Lanthanide-Mannose Complex, *Adv. Sci.*, 2019, **6**, 1802112.

28 G. Weng, S. Thanneeru and J. He, Dynamic Coordination of Eu-Iminodiacetate to Control Fluorochromic Response of Polymer Hydrogels to Multistimuli, *Adv. Mater.*, 2018, **30**, 1706526.

29 Z. Li, G. Wang, Y. Ye, B. Li, H. Li and B. Chen, Loading Photochromic Molecules into a Luminescent Metal-Organic Framework for Information Anticounterfeiting, *Angew. Chem., Int. Ed.*, 2019, **58**, 18025–18031.

30 J. Wang, S. Sun, B. Wu, L. Hou, P. Ding, X. Guo, M. A. Cohen Stuart and J. Wang, Processable and Luminescent Supramolecular Hydrogels from Complex Coacervation of Polycations with Lanthanide Coordination Polyanions, *Macromolecules*, 2019, **52**, 8643–8650.

31 S. Wei, W. Lu, X. Le, C. Ma, H. Lin, B. Wu, J. Zhang, P. Theato and T. Chen, Bioinspired Synergistic Fluorescence-Color-Switchable Polymeric Hydrogel Actuators, *Angew. Chem., Int. Ed.*, 2019, **58**, 16243–16251.

32 X. Xu, J. Wang and B. Yan, Facile Fabrication of Luminescent Eu(III) Functionalized HOF Hydrogel Film with Multifunctionailities: Quinolones Fluorescent Sensor and Anticounterfeiting Platform, *Adv. Funct. Mater.*, 2021, **31**, 2103321.

33 A. Cayuela, S. R. Kennedy, M. L. Soriano, C. D. Jones, M. Valcarcel and J. W. Steed, Fluorescent carbon dot-molecular salt hydrogels, *Chem. Sci.*, 2015, **6**, 6139–6146.

34 X. Y. Du, C. F. Wang, G. Wu and S. Chen, The Rapid and Large-Scale Production of Carbon Quantum Dots and their Integration with Polymers, *Angew. Chem., Int. Ed.*, 2021, **60**, 8585–8595.

35 S. Wu, H. Shi, W. Lu, S. Wei, H. Shang, H. Liu, M. Si, X. Le, G. Yin, P. Theato and T. Chen, Aggregation-Induced Emissive Carbon Dots Gels for Octopus-Inspired Shape/Color Synergistically Adjustable Actuators, *Angew. Chem. Int. Ed.*, 2021, **60**, 21890–21898.

36 Y. Zhang, Y. Zhao, D. Wu, J. Xue, Y. Qiu, M. Liao, Q. Pei, M. S. Goorsky and X. He, Homogeneous Freestanding Luminescent Perovskite Organogel with Superior Water Stability, *Adv. Mater.*, 2019, **31**, e1902928.

37 J. Qi, H. Ou, Q. Liu and D. Ding, Gathering brings strength: How organic aggregates boost disease phototheranostics, *Aggregate*, 2021, **2**, 95–113.

38 J. Li, H. Gao, R. Liu, C. Chen, S. Zeng, Q. Liu and D. Ding, Endoplasmic reticulum targeted AIE bioprobe as a highly efficient inducer of immunogenic cell death, *Sci. China: Chem.*, 2020, **63**, 1428–1434.

39 D. Chen, Z. Wang, H. Dai, X. Lv, Q. Ma, D. P. Yang, J. Shao, Z. Xu and X. Dong, Boosting $O2^{\bullet-}$ Photogeneration *via* Promoting Intersystem-Crossing and Electron-Donating Efficiency of Aza-BODIPY-Based Nanoplatforms for Hypoxic-Tumor Photodynamic Therapy, *Small Methods*, 2020, **4**, 2000013.

40 X. Shi, S. H. P. Sung, J. H. C. Chau, Y. Li, Z. Liu, R. T. K. Kwok, J. Liu, P. Xiao, J. Zhang, B. Liu, J. W. Y. Lam and B. Z. Tang, Killing G(+) or G(−) Bacteria? The Important Role of Molecular Charge in AIE-Active Photosensitizers, *Small Methods*, 2020, **4**, 2000046.

41 W. Lu, S. Wei, H. Shi, X. Le, G. Yin and T. Chen, Progress in aggregation-induced emission-active fluorescent polymeric hydrogels, *Aggregate*, 2021, **2**, e37.

42 Y. Tu, Z. Zhao, J. W. Y. Lam and B. Z. Tang, Aggregate Science: Much to Explore in the Meso World, *Matter*, 2021, **4**, 338–349.

43 J. Yang, M. Fang and Z. Li, Organic luminescent materials: The concentration on aggregates from aggregation-induced emission, *Aggregate*, 2020, **1**, 6–18.

44 Y. Yang, Q. Li, H. Zhang, H. Liu, X. Ji and B. Z. Tang, Codes in Code: AIE Supramolecular Adhesive Hydrogels Store Huge Amounts of Information, *Adv. Mater.*, 2021, **33**, e2105418.

45 P. Li, D. Zhang, Y. Zhang, W. Lu, J. Zhang, W. Wang, Q. He, P. Theato and T. Chen, Aggregation-Caused Quenching-Type Naphthalimide Fluorophores Grafted and Ionized in a 3D Polymeric Hydrogel Network for Highly Fluorescent and Locally Tunable Emission, *ACS Macro Lett.*, 2019, **8**, 937–942.

46 H. Liu, S. Wei, H. Qiu, B. Zhan, Q. Liu, W. Lu, J. Zhang, T. Ngai and T. Chen, Naphthalimide-Based Aggregation-Induced Emissive Polymeric Hydrogels for Fluorescent Pattern Switch and Biomimetic Actuators, *Macromol. Rapid Commun.*, 2020, **41**, e2000123.

47 S. Wei, Z. Li, W. Lu, H. Liu, J. Zhang, T. Chen and B. Z. Tang, Multicolor Fluorescent Polymeric Hydrogels, *Angew. Chem., Int. Ed.*, 2021, **60**, 8608–8624.
48 R. M. Duke, E. B. Veale, F. M. Pfeffer, P. E. Kruger and T. Gunnlaugsson, Colorimetric and fluorescent anion sensors: an overview of recent developments in the use of 1,8-naphthalimide-based chemosensors, *Chem. Soc. Rev.*, 2010, **39**, 3936–3953.
49 P. Gopikrishna, N. Meher and P. K. Iyer, Functional 1,8-Naphthalimide AIE/AIEEgens: Recent Advances and Prospects, *ACS Appl. Mater. Interfaces*, 2018, **10**, 12081–12111.